Estimation of Target Detectability for Maritime Target Tracking in the PDA Framework

Erik F. Wilthil*, Yaakov Bar-Shalom†, Peter Willett† and Edmund Brekke*
* Department of Engineering Cybernetics, NTNU, Trondheim, Norway.
Email: {erik.wilthil, edmund.brekke}@ntnu.no
† Department of Electrical and Computer Engineering, University of Connecticut, Storrs, CT, USA.
Email: {yaakov.bar-shalom, peter.willett}@uconn.edu

***Abstract*—The detection probability of maritime vessels may change over time, either slowly or more abruptly, due to effects such as sea state and varying aspect angle. If the varying detectability is not accounted for in the tracking system, tracks may be terminated or lost. The undetected targets may cause dangerous situations in applications such as maritime collision avoidance. In the following, we propose two methods for tracking targets with varying detection probability, both in the integrated probabilistic data association (IPDA) framework. One method uses the number of validated measurements to estimate the detectability of the target, while the other calculates the joint detectability and existence probabilities based on the measurement association likelihoods. Both methods show significant improvements over the conventional Markov chain 1 and 2 IPDAs.**

I. Introduction

With increased autonomy in the maritime domain, reliable situational awareness and collision avoidance capabilities are needed to ensure the safe operation of vessels. Although many vessels are equipped with automatic identification system (AIS) transponders, a good object detection and tracking system is also needed to track targets without AIS, such as kayaks and leisure craft, or as a backup to the AIS system.

The main priority of tracking systems for collision avoidance is the capability to quickly and reliably track targets, as an undetected target is a direct threat to safety. This is also the case when confirmed tracks on targets are terminated, as the collision avoidance system may decide to steer into the now untracked target's path. However, false tracks may induce unnecessary maneuvers from the collision avoidance system and cause dangerous situation from other ships, and the system should also be able to terminate false tracks quickly.

The literature on track management for fluctuating detection probability is sparse. In [2], it was found that a Shiryaev test can greatly improve track termination performance when the detection probability is varying. In [10], the authors use a particle filter-based approach to estimate the detection probability, where the particle filter handles the nonlinearities that arise when the detection probability is constrained to a limited interval. Ref. [12] presents an adaptive tracker that is able to estimate the detection probability using a belief propagation message passing scheme. A method for extending random finite set (RFS) filters to include the detection probability in the state vector is presented in [6], with results in [7]. The resulting filters performs well with a constant, but unknown, detection probability.

The first contribution of this paper is an experimental investigation of whether the variations in small vessel detectability can be adequately modeled by varying aspect angle, based on a dataset from a collision avoidance test. The motivation for using a Markov model as in e.g. [2], [10] is that it is difficult to identify the primary contributing factor to the detectability variations, and we will investigate if this is the case for this dataset as well.

The second contribution of this paper is the extension of the integrated probabilistic data association (IPDA) to handle varying target detectability. The first extension estimates the detectability based on the number of validated measurements, and the second calculates the joint detection and existence probability. We have chosen the probabilistic data association (PDA) framework for two main reasons. The first is that the PDA has proven to be an efficient tool for object detection and tracking in short-range maritime collision avoidance, see e.g. [16], [5], [4], [11]. The other is that the IPDA is a special case of the joint integrated probabilistic data association (JIPDA) [8], which in turn can be derived from Poisson multi-Bernoulli mixture (PMBM) filters [14].

The rest of the paper is structured as follows. Section II contains assumptions and motivation, Section III describes the modifications made to the IPDA in order to account for varying detectability, Section IV presents the results, and the conclusion follows in Section V.

II. Motivation and problem formulation

A. Definitions

The goal of the system is to estimate the state of the target at time k, which consists of a kinematic component x_k with target position and velocity, and the detection probability d_k. Measurements are denoted z_k^i, $Z_k = \{z_k^i\}_{i=0}^{m_k}$ and $Z^k = (Z_{k_0}, \dots, Z_k)$ for measurements, sets of measurements and data (sequence of sets) at time k, respectively.

Assumption 1: The target moves according to

$$p(x_{k+1}|x_k) = \mathcal{N}(x_{k+1}; F_k x_k, Q_k) \tag{1}$$

independent for all k, and $\mathcal{N}(x; \hat{x}, P)$ is the probability density function (PDF) of the normal distribution of x, with expected value $\hat{x}$ and covariance P, respectively.

Assumption 2: The target is assumed to have time-varying detectability, chosen from a discrete set of N_d states. Let E_k^j be the event that the target is in detectability mode j at time k, i.e. that $d_k = P_D^j$. Further, assume that the values of P_D^j are known, and that d follows a random process according to

$$P(E_k^j|E_{k-1}^i) = \pi_{ij} \qquad i,j = 1,\dots,N_d \tag{2}$$

Assumption 3: The target-originated measurement is distributed according to

$$p(z_k|x_k) = \mathcal{N}(z_k; Hx_k, R_k) \tag{3}$$

independently for all k, and independent of Assumption 1. The target is detected with probability P_D^j, according to the current detectability mode.

Assumption 4: The number of false alarms in the surveillance region follows a Poisson distribution, with probability mass function (PMF)

$$\mu_F(m) = \frac{(\lambda V)^m}{m!} e^{-\lambda V} \tag{4}$$

where V is the area of the surveillance region, and λ is the clutter density. The spatial distribution of clutter measurements is assumed to be uniform.

Assumption 5: Target existence at time k is denoted $\mathcal{H}_k$, and $\bar{\mathcal{H}}_k$ is defined as the complementary event, namely that the target does not exist at time k. It is assumed to follow a Bernoulli random process according to

$$P(\mathcal{H}_k|\mathcal{H}_{k-1}) = p_s \tag{5}$$

$$P(\mathcal{H}_k|\bar{\mathcal{H}}_{k-1}) = p_b \tag{6}$$

where p_s and p_b are the probability of survival and birth, respectively.

B. Track initiation with constant detectability

As one of the assumptions of PDA is that it cannot begin before a track has been initialized, some form of track initialization is needed. Fundamental to the PDA approach is the calculation of the association probabilities for the validated measurements at the current time based on a single prior. For the m_k validated measurements, let θ_k^i be the event that measurement z_k^i is the target-originated measurement for $i = 1,\dots,m_k$, and that none of the measurements are target-originated for $i = 0$. One of the first attempts at handling track initiation in the PDA framework can be found in [3], where an additional association event is added, the event that the target is unobservable. This causes tracks that have a low probability of being observable to have low association probabilities for measurements in the validation gate, reducing their impact on the posterior state estimate. However, the probability of detection is still considered constant in [3] when the target is detectable.

Other approaches to track initiation are logic-based track formation [1] and sequential tests [13], [15]. This includes the popular M/N-logic, which requires M detections in N scans in order to confirm the track. This approach only accounts for the detectability of the target implicitly by the choice of M and N. As explored in [2], this may have a significant impact on performance when the detectability of the target changes. The detection probability also appears in the likelihood ratio in the sequential probability ratio test (SPRT) of [13].

In the following, we will focus on the IPDA described in [9]. As opposed to [3], where the PDA association probabilities are modified with an extra event, the evaluation of the association event probabilities are the same as in the original treatment of the PDA, and the existence probability of the target is calculated by

$$P(\mathcal{H}_k|Z^k) = \frac{\mathcal{L}_k P(\mathcal{H}_k|Z^{k-1})}{1-(1-\mathcal{L}_k)P(\mathcal{H}_k|Z^{k-1})} \tag{7}$$

where $\mathcal{L}_k$ is the likelihood ratio of the target-present versus the clutter-only hypotheses, based on the measurements in scan k. Under the PDA assumption, this is given by

$$\mathcal{L}_k = 1 - P_D P_G + P_D \lambda^{-1} \sum_{i=1}^{m_k} p(z_k^i|\theta_k^i, Z^{k-1}) \tag{8}$$

where P_G is the validation gate probability and $p(z_k^i|\theta_k^i, Z^{k-1}) = \mathcal{N}(\nu_k^i; 0, S_k)$. The innovations are given by $\nu_k^i = z_k^i - H\hat{x}_{k|k-1}$, with corresponding covariance S_k. The time update of the existence probability is given by

$$P(\mathcal{H}_k|Z^{k-1}) = p_s P(\mathcal{H}_{k-1}|Z^{k-1}) + p_b P(\bar{\mathcal{H}}_{k-1}|Z^{k-1}). \tag{9}$$

This variant is denoted the Markov chain one (MC1) IPDA in [9]. It is also derived with another Markov chain, named the Markov chain two (MC2) IPDA. In addition to the target-present and no-target state, it also includes an undetectable-target state. The likelihoods of undetectable targets cannot be distinguished from the clutter-only hypothesis in the MC2 IPDA, which means that erroneous tracks will have a high existence probability several scans after the track is lost.

The one-point initialization procedure [1] is used for forming preliminary tracks, with existence probability ε_I. If the existence probability exceeds a threshold ε_C, the track is confirmed. Tracks with existence probability below ε_T are terminated. Established tracks are gated according to known techniques, with gate probability P_G [1]. Any measurements that are gated by confirmed tracks are not used to update preliminary tracks, and new preliminary tracks are formed only with measurements that are not gated by confirmed or preliminary tracks.

C. Forensic analysis of recorded data

Varying target detectability may have many sources, such as target aspect angle, range and varying sea state. A scenario where target detectability is an issue is shown in Fig. 1, which shows data from a collision avoidance experiment conducted in the Trondheimsfjord in September 2018. There are three targets present in the tests, two boats and a stationary seamark[1]. The target moving east-to-west is a tugboat with

[1]A seamark is an aid to navigation for passing ships, typically a board or a buoy attached to the sea floor.

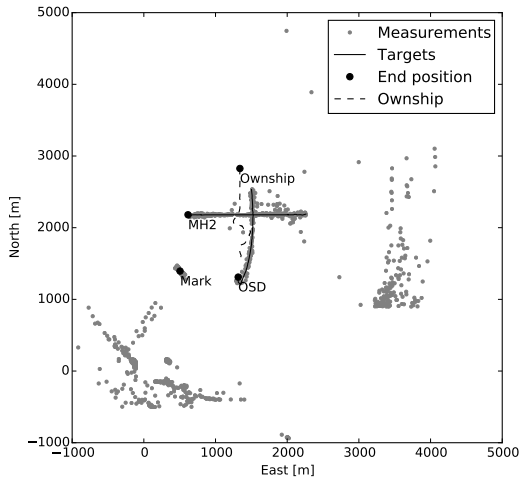

Fig. 1. Scenario overview. The grey dots are radar measurements, the black lines are AIS position trajectories, and the dashed line is the ownship position trajectory.

Fig. 2. The targets present in the experiments. Top left: The Ocean Space Drone. Bottom left: Munkholmen II. Right: The seamark.

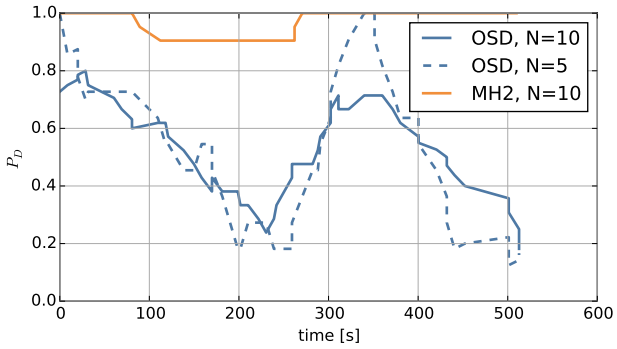

Fig. 3. Empirical detection probability for the two boats in Fig. 1, calculated by (10), where the values close to the start and end of the dataset have been calculated by truncating (10).

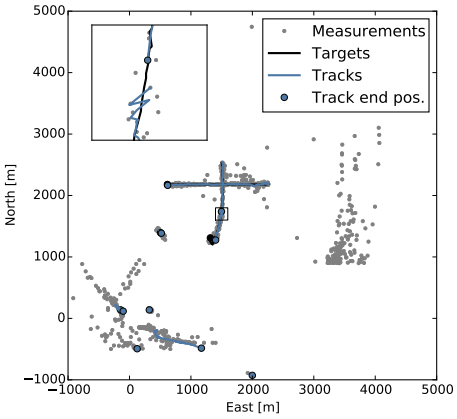

Fig. 4. Resulting tracks after running the IPDA tracker described in Section II-A. The track from the OSD target is terminated due to the assumed high detection probability, as shown in the inset.

callsign Munkholmen II (MH II), which has a steel hull. The target moving north-to-south is a lifeboat, repurposed into an autonomous test vessel, with callsign Ocean Space Drone (OSD). It has a fiberglass hull. A radar is mounted on the ownship, which successfully avoids collision with both targets. The targets are shown in Fig. 2. The dataset has a low amount of clutter, with the exception of near-shore areas close to the origin and to the east.

In the following discussion, the ground truth is based on the AIS-indicated position of the targets, and the measurements recorded during the experiments. Although the AIS system is based on satellite navigation with its own flaws, we believe it to be of sufficient accuracy to discuss the issues presented in the rest of this section.

Both targets have frequent detections for the most part, but there are some periods with more sparse detections. By assuming the AIS-indicated position is sufficiently accurate and a low clutter density, a validation gate can be set up around the reported position. Let δ_k be a measurement indicator, which is 0 when the validation gate is empty at time k, and 1 otherwise. Then, the moving average detection probability can be calculated by

$$P_D(k) = \frac{1}{2N+1} \sum_{n=k-N}^{k+N} \delta_n. \tag{10}$$

Fig. 3 shows the detection probability for each of the targets with different values of N.

The MH II has very good reflective properties and has a high detection probability throughout the experiment, but the detection probability of the OSD varies a lot. Keeping a continuous track on the OSD is hard, and Fig. 4 shows a set of tracks resulting from running an IPDA described in Section II-A with a detection probability of 0.8. The track on the OSD is lost and regained during the experiment.

In addition to the dataset shown in Figures 1 and 4, an additional 15 datasets have been analysed. These datasets comprise 3554 radar scans of the targets from 2 hours and 50 minutes of data, collected the same day as the previously discussed

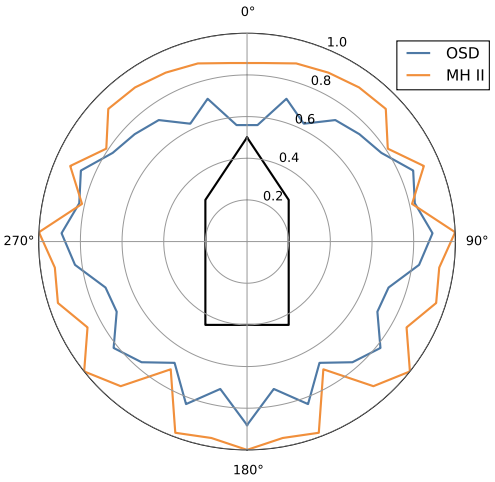

Fig. 5. Empirical detection probability based on the AIS-indicated aspect angle. Zero degrees is the bow. Symmetry about the centerline is assumed, and the range to the targets have not been accounted for.

scenario. The goal is to investigate whether the aspect angle is a main contributing factor to the varying detection probability. For every timestep k, a validation gate is set up around the AIS-indicated position, and δ_k is evaluated. Additionally, the aspect angle is calculated based on the velocity information of the target, also given by the AIS system. The aspect angle α can be found from the angle between the vectors from the target to the ownship and the velocity of the target, and is given by

$$\cos\alpha_k = \frac{p_k^{to} \cdot v_k^t}{\|p_k^{to}\|\|v_k^t\|} \tag{11}$$

where p_k^{to} is the vector from the target to the ownship position, and v_k^t is the target velocity. The accumulated aspect angle and detection indicators are then used to evaluate the aspect-dependent detection probability by dividing the ship aspect angle into discrete bins, and the detection probability for each bin is calculated by

$$P_D = \frac{\sum_{\ell=1}^{N} \delta_\ell}{N}. \tag{12}$$

The results based on all the datasets are shown in Fig. 5, where it has been assumed that the target is symmetric about the centerline to increase the number of samples per bin. The steel hull of MH II has good detectability from all aspect angles, around $P_D = 0.9$. The OSD is slightly less detectable, usually about 0.8 and as low as 0.6 from the front. However, there are no aspect angles with a detection probability which is as low as the ones indicated in Fig. 3. This example shows that it can be hard to model the detectability by a single parameter, and justifies the use of a random process as in Assumption 2 for these datasets.

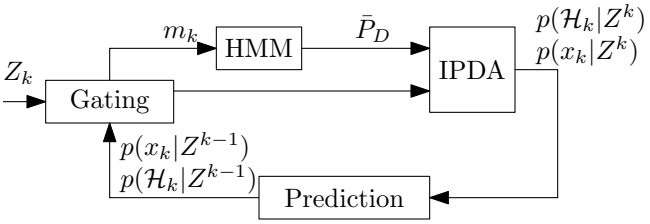

Fig. 6. The cascade form HMM and IPDA estimators.

III. Extensions to the IPDA

In the following two sections, we introduce two extensions which accounts for varying target detectability.

A. Cascade form HMM and IPDA

This method consists of a hidden Markov model (HMM) to estimate the detectability of the target based on the number of measurements in the validation gate, and the actual measurements Z_k are not used. A MC1-IPDA is used to estimate the target existence probability based on the detectability estimate $\bar{P}_D$. This structure is shown in Fig. 6.

To estimate the detectability of the target, the number of measurements in the validation gate m_k and the gate area V_k are evaluated when the validation gate is setup. Under the Poisson clutter assumption and detectability mode E_k^j, m_k has the distribution

$$P(m_k|E_k^j, \mathcal{H}_k) = \mu_F(m_k)(1 - P_D^j P_G) + \mu_F(m_k - 1)P_D^j P_G \tag{13}$$

where the first term is the probability of m_k clutter measurements and a missed detection, and the second term is the probability of $m_k - 1$ clutter measurements and a detection, respectively. Given a sequence of observations $m^k = (m_{k_0}, \ldots, m_k)$, the probability of being in mode j can be calculated recursively by

$$P(E_k^j|m^k, \mathcal{H}_k) = \frac{1}{c} P(m_k|E_k^j, m^{k-1}, \mathcal{H}_k) P(E_k^j|m^{k-1}, \mathcal{H}_{k-1}) \tag{14}$$

where $c = P(m_k|m^{k-1})$ is a normalization constant. As the detections and clutter are independent over time, $P(m_k|E_k^j, m^{k-1}) = P(m_k|E_k^j)$, and

$$P(E_k^j|m^k, \mathcal{H}_k) = \frac{1}{c} P(E_k^j|m^k, \mathcal{H}_k) \cdot \sum_{i=1}^{N_d} \pi_{ij} P(E_{k-1}^i|m^{k-1}, \mathcal{H}_k). \tag{15}$$

The estimate of the detection probability is then given by

$$\bar{P}_D = \sum_{j=1}^{N_d} P_D^j P(E_k^j|m_k, \mathcal{H}_k) \tag{16}$$

which is then used in a regular IPDA, as described in Section II-B.

Although calculating the average detectability in this way is a heuristic technique, the following example illustrates

how the approximation fits into the PDA framework. Consider the probabilities of the measurement association events $p(\theta_k^i|m_k, \mathcal{H}_k, Z^{k-1})$. By marginalizing over the detectability, this becomes

$$P(\theta_k^i|m_k) = \sum_{j=1}^{N_d} P(\theta_k^i|E_k^j, m_k)P(E_k^j|m_k) \tag{17}$$

where the conditioning on target existence $\mathcal{H}_k$ and past data Z^{k-1} has been omitted for brevity. The first term is the regular PDA association event probability with detection probability equal to P_D^j, and the second term is the HMM probability of being in mode j. For the nonparametric PDA, this gives

$$\begin{aligned} P(\theta_k^i|m_k) &= \begin{cases} \sum_{j=1}^{N_d}(1 - P_G P_D^j)P(E_k^j|m_k) & i = 0 \\ \sum_{j=1}^{N_d} \frac{P_G P_D^j}{m_k} P(E_k^j|m_k) & i = 1, \dots, m_k \end{cases} \\ &= \begin{cases} 1 - P_G \bar{P}_D & i = 0 \\ \frac{P_G \bar{P}_D}{m_k} & i = 1, \dots, m_k \end{cases} \end{aligned} \tag{18}$$

which are expressions from the prior PDA probabilities using the value $\bar{P}_D$.

B. Detectability-based IPDA

The estimation of the detectability state can also be integrated into the IPDA presented in Section II-B, such that the detectability is estimated based on the likelihood of the measurement association hypothesis. The goal of this extension is to estimate the joint probability of target existence $\mathcal{H}_k$ and detectability mode E_k^j, given by

$$P(\mathcal{H}_k, E_k^j|Z^k) = \frac{p(Z_k|\mathcal{H}_k, E_k^j, Z^{k-1})}{p(Z_k|Z^{k-1})} P(\mathcal{H}_k, E_k^j|Z^{k-1}). \tag{19}$$

where the dependence on the number of measurements m_k can be made explicit by

$$\begin{aligned} p(Z_k|E_k^j, \mathcal{H}_k, Z^{k-1}) =& p(Z_k|m_k, E_k^j, \mathcal{H}_k, Z^{k-1}) \\ & \cdot P(m_k|E_k^j, \mathcal{H}_k, Z^{k-1}) \end{aligned} \tag{20}$$

where the last term is given in (13) since it is independent of the past data Z^{k-1}. By considering the different data association hypotheses θ_k^i, we have

$$\begin{aligned} p(Z_k|m_k, E_k^j, \mathcal{H}_k, Z^{k-1}) =& \sum_{i=0}^{m_k} p(Z_k|\theta_k^i, m_k, E_k^j, \mathcal{H}_k, Z^{k-1}) \\ & \cdot P(\theta_k^i|m_k, E_k^j, \mathcal{H}_k, Z^{k-1}) \end{aligned} \tag{21}$$

where the PDF of the measurements can be found in e.g. [1], and are given by

$$\begin{aligned} & p(Z_k|\theta_k^i, m_k, E_k^j, \mathcal{H}_k, Z^{k-1}) \\ &= \begin{cases} V_k^{-m_k+1} P_G^{-1} \mathcal{N}(\nu_k^i; 0, S_k) & i = 1, \dots, m_k \\ V_k^{-m_k} & i = 0 \end{cases}. \end{aligned} \tag{22}$$

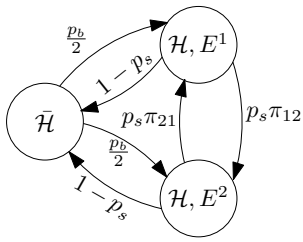

Fig. 7. The Markov chain with the nonexisting target-state, and two detectability states. The self-transition probabilities are not shown.

Conditioned on target existence and detectability, the prior association event probabilites can be found from the regular PDA equations, and are also found in e.g. [1]:

$$\begin{aligned} & P(\theta_k^i|m_k, E_k^j, \mathcal{H}_k, Z^{k-1}) \\ &= \begin{cases} \frac{1}{m_k} P_D^j P_G c_j^{-1} & i = 1, \dots, m_k \\ (1 - P_D^j P_G) \frac{\mu_F(m_k)}{\mu_F(m_k - 1)} c_j^{-1} & i = 0 \end{cases} \end{aligned} \tag{23}$$

where c_j normalizes the association events. (13) divided by c_j can be shown to be $\mu_F(m_k - 1)$, and summing and multiplying everything together into (20) gives

$$\begin{aligned} p(Z_k|E_k^j, \mathcal{H}_k, Z^{k-1}) &= \mu_F(m_k) V_k^{-m_k}(1 - P_D^j P_G) \\ &+ \mu_F(m_k - 1) V_k^{m_k - 1} \frac{1}{m_k} P_D^j \sum_{i=1}^{m_k} \mathcal{N}(\nu_k^i; 0, S_k). \end{aligned} \tag{24}$$

Inserting the clutter PMF from Assumption 4 into (24), cancelling and gathering terms yields

$$\begin{aligned} p(Z_k|E_k^j, \mathcal{H}_k, Z^{k-1}) = \frac{\lambda^{m_k} e^{-\lambda V_k}}{m_k!} \Big[& (1 - P_D^j P_G) \\ & + P_D^j \lambda^{-1} \sum_{i=1}^{m_k} \mathcal{N}(\nu_k^i; 0, S_k) \Big] = C_k \mathcal{L}_k^j \end{aligned} \tag{25}$$

where $\mathcal{L}_k^j$ is the likelihood ratio of the measurements in scan k for the target present in detectability mode j versus the clutter-only hypotheses, as in (8).

The prior $P(\mathcal{H}_k, E_k^j|Z^{k-1})$ is calculated as follows. Since the detectability mode change conditioned on target existence is known from Assumption 2, it is rewritten as (omitting the dependence on the past data Z^{k-1} for brevity)

$$\begin{aligned} P(\mathcal{H}_k, E_k^j) &= P(E_k^j, \mathcal{H}_k|\mathcal{H}_{k-1})P(\mathcal{H}_{k-1}) \\ &+ P(E_k^j, \mathcal{H}_k|\bar{\mathcal{H}}_{k-1})P(\bar{\mathcal{H}}_{k-1}) \\ &= p_s \sum_{i=1}^{N_d} \pi_{ij} P(E_{k-1}^i, \mathcal{H}_{k-1}) + \frac{p_b}{N_d} P(\bar{\mathcal{H}}_{k-1}) \end{aligned} \tag{26}$$

These transition probabilities are equivalent to a Markov chain with the $N_d + 1$ states $\bar{\mathcal{H}}$ and $(\mathcal{H}, E^j)$ for $j = 1$ to N_d. An example with two detectability states is shown in Fig. 7.

The denominator of (19) is a normalization constant which can be found by summing over the possible target hypotheses, given by

$$\begin{aligned} p(Z_k|Z^{k-1}) &= p(Z_k|\bar{\mathcal{H}}_k, Z^{k-1})P(\bar{\mathcal{H}}_k|Z^{k-1}) \\ &\quad + \sum_{j=1}^{N_d} p(Z_k|\mathcal{H}_k, E_k^j, Z^{k-1})P(\mathcal{H}_k, E_k^j|Z^{k-1}) \\ &= C_k \left(1 - \sum_{j=1}^{N_d} (1 - \mathcal{L}_k^j) P(\mathcal{H}_k, E_k^j|Z^{k-1}) \right) \end{aligned} \tag{27}$$

and the C_k cancels in (19) with the same term in (25). To summarize, the time update of the IPDA with detectability estimation is given by a Markov chain as shown in Fig. 7, and the measurement update is given by

$$P(\mathcal{H}_k, E_k^j|Z^k) = \frac{\mathcal{L}_k^j P(\mathcal{H}_k, E_k^j|Z^{k-1})}{1 - \sum_{i=1}^{N_d}(1 - \mathcal{L}_k^i) P(\mathcal{H}_k, E_k^i|Z^{k-1})}. \tag{28}$$

The MC1- and MC2-IPDAs from [9] can be obtained from this general expression by assuming a single mode with detection probability P_D or two detectability modes with detection probabilities of P_D and 0, respectively.

IV. Results

The two trackers that account for varying target detectability will be compared with the Markov chain 1 and 2 IPDAs. The four trackers can be summarized as follows:

MC1-IPDA
: The Markov Chain 1 IPDA without detectability estimation. It has a single detection probability P_D^H.

MC2-IPDA
: The Markov Chain 2 IPDA that allows for undetectable targets. It also has a single detection probability P_D^H.

HMM-IPDA
: The Markov Chain 1 IPDA with detectability estimation provided by a HMM. The HMM has two detection probability values, P_D^H and P_D^L.

DET-IPDA
: The IPDA with joint detectability and target existence estimation, with two detection probability values, P_D^H and P_D^L.

Apart from the detectability models, the trackers use the same parameters, given in Table I. For the MC2-IPDA and DET-IPDA, the target existence probability is the summed existence probability of the two detectability modes.

All of the trackers use the same motion model, a white noise acceleration model given by

$$F_k = \begin{bmatrix} 1 & T \\ 0 & 1 \end{bmatrix} \qquad Q = q \begin{bmatrix} T^4/4 & T^3/2 \\ T^3/2 & T^2 \end{bmatrix} \tag{29}$$

independent for the north- and east dimensions with sample time T. Cartesian position measurements are used, with covariance rI_2, where I_2 is the identity matrix.

TABLE I
Simulation parameters

Parameter	Value
Sample time T	$3\,\mathrm{s}$
Detection probabilities P_D^H, P_D^L	0.8, 0.3
Clutter density λ	$1 \times 10^{-5}\,\mathrm{m}^{-2}$
Measurement covariance r	$100\,\mathrm{m}^2$
Process noise covariance q	$0.025\,\mathrm{m}^2\,\mathrm{s}^{-4}$
Survival probability p_s	1.0
Birth probability p_b	0
Detectability mode change probability π_{ij}	0.8, $i = j$ 0.2, $i \neq j$
Initial existence probability ε_I	0.2
Confirmation threshold ε_C	0.99
Termination threshold ε_T	0.1
Number of simulations N_{MC}	2500

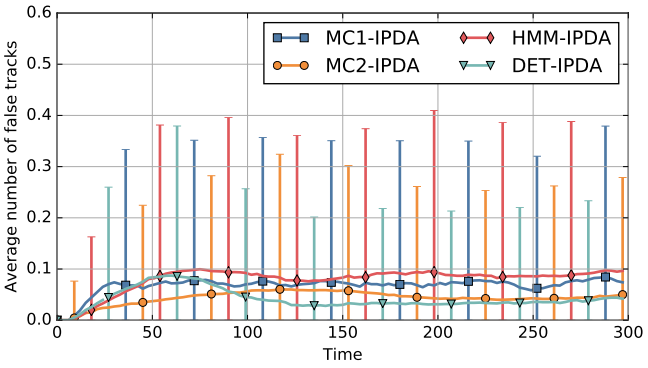

Fig. 8. Average number of confirmed tracks for the clutter-only scenario. Error bars correspond to one standard deviation.

A. False tracks

It is expected that allowing targets to have a lower detection probability in a surveillance area will increase the number of false tracks. In this section, we investigate if this expectation holds true, and to what extent it affects the tracking system.

To test the false track rejection capabilities of the trackers, a square surveillance area with edge length $2\,\mathrm{km}$ is set up, and clutter is generated according to Assumption 4 with clutter density λ given in Table I. No targets are present. Fig. 8 shows the average number of confirmed tracks over N_{MC} simulations.

The premise that the trackers with lower detectability are prone to more false tracks does not have merit as they all have a similar number of false tracks. The DET-IPDA and MC2-IPDA have a slightly lower number than the other two, but the results are still comparable when considering the sample standard deviation. The reason for this is that the trackers account for the lower detection probability in the update of the target existence probability. However, there is a large difference in the average duration of the false tracks, as summarized in Table II. The MC1-IPDA is very fast in both track initiation and termination, and the MC2-IPDA is very slow. When tracks persist for a long time, it will gate measurements that may have been used to confirm another

TABLE II
FALSE TRACK DURATION

Tracker	Avg. duration	Avg. conf. time
MC1-IPDA	10.0 scans	4.8 scans
MC2-IPDA	78.5 scans	15.8 scans
HMM-IPDA	29.3 scans	10.1 scans
DET-IPDA	30.4 scans	7.7 scans

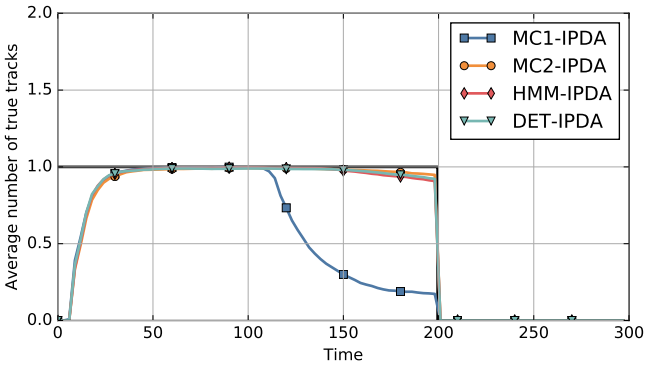

Fig. 9. Average number of true tracks with a single target present. The black line shows the ground truth. The detectability of the target drops at $t = 100\,\mathrm{s}$.

track, which in part may explain the lower average number of false tracks in the DET-IPDA and MC2-IPDA. These also have a slightly lower standard deviation in the number of false tracks.

B. Detectability estimation and lost tracks

To test the capability of tracking a target with varying detectability, a single target is added to the surveillance region previously described. It starts in the high detectability-mode, and changes to the low detectability-mode after $100\,\mathrm{s}$. After an additional $100\,\mathrm{s}$, the target disappears, and the scenario continues for an additional $100\,\mathrm{s}$. The purpose of the change in the detectability and track existence is to test both the ability to track targets with reduced detectability, and track termination capabilities, i.e. how fast the track is terminated when it is lost.

More precisely, define a true track as a confirmed track that has a position error of less than $100\,\mathrm{m}$. Further, a lost track is defined as a previously confirmed track that no longer satisfied this requirement. Consequently, a confirmed track that manages to track the target until it disappears will be considered lost until it is terminated. For each tracker, the average number of true tracks are shown in Fig. 9, and the average number of lost tracks are shown in Fig. 10.

As expected, the IPDA with constant detection probability struggles to keep track of the target when the detectability decreases. However, the fast track termination capabilities ensures the tracks are terminated rather than lost. The tracks that are maintained until the target disappears are also terminated very quickly. The other three trackers are much better at tracking the target until it disappears. The MC2-IPDA,

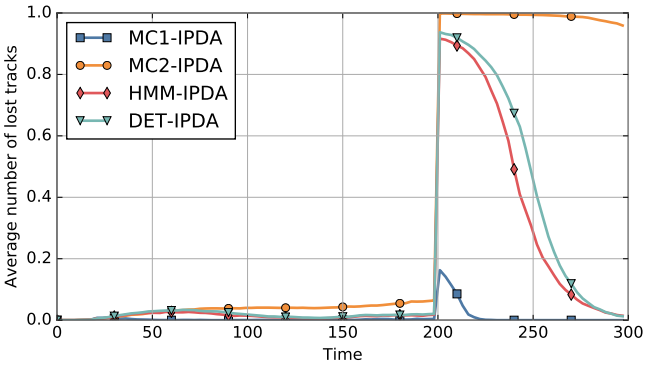

Fig. 10. Number of lost tracks with a single target present.

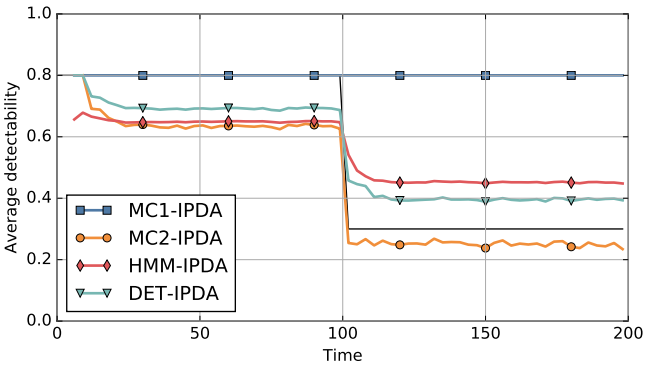

Fig. 11. Average mode of the detectability estimate of confirmed tracks when the target is present. The black line shows the ground truth.

however, still maintains over 90% of the lost tracks for more than 30 scans after the target disappears. The HMM-IPDA and the DET-IPDA terminates nearly all of the lost tracks before the end of the scenario.

The average mode of the detectability estimate is shown in Fig. 11. The DET-IPDA esitmates the detectability of the target slightly better than the HMM-IPDA. When the detectability is lowered, the MC2-IPDA is the closest, as one of the modes allows for detectability lower than the true value.

C. Real data results

We now test the trackers on the motivating scenario presented in Section II-C with 3 targets (OSD, MH II and the seamark). The tracking system parameters are the same as in Table I, with some exceptions. The sampling interval varies slightly according to when data is received, and the average is $2.88\,\mathrm{s}$. The clutter density is not known, and nonparametric tracking methods are used by substituting $\lambda = m_k/V_k$ where m_k and V_k are the number of validated measurements and the area of the validation gate, respectively. The Cartesian position measurement model is still used, but the measurement covariance is calculated by a polar to Cartesian conversion [1] with polar measurement standard deviations of $20\,\mathrm{m}$ and $2.3°$. Further details on the radar data processing can be found in

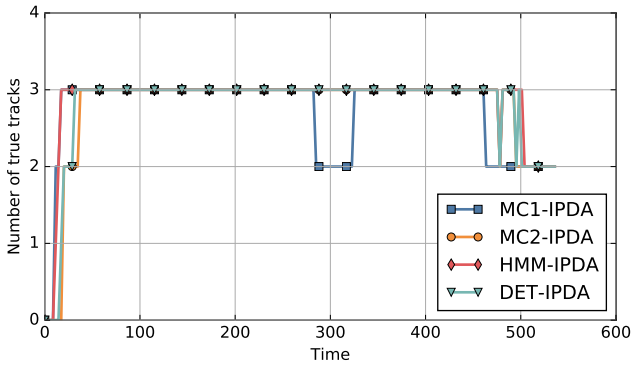

Fig. 12. Number of true tracks for the tracking methods in the real data scenario.

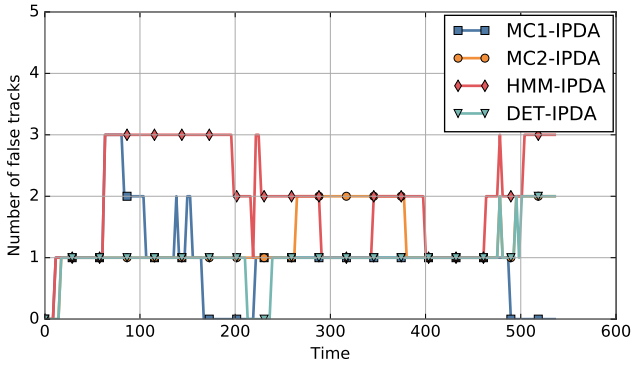

Fig. 13. Number of false targets for the tracking methods in the real data scenario.

[16], [15]. The limit for declaring a true track is now reduced to $60\,\mathrm{m}$.

The number of true and false tracks can be seen in Fig. 12 and Fig. 13, respectively. The MC1-IPDA loses the track of the OSD from $t = 280\,\mathrm{s}$ to $t = 320\,\mathrm{s}$, and the other trackers are able to keep track. The MC2- and DET-IPDA are slightly slower at confirming the track on the drone. Both the MC1- and HMM-IPDA rapidly confirms three false tracks, close to the island at the origin. The MC1-IPDA terminates these quickly, but the HMM-IPDA maintains them for a while longer. Both the MC2-IPDA and the DET-IPDA outperform the two other methods with respect to false tracks. At the end of the test, the OSD makes a 180° turn, and the trackers either lose or terminate the track.

V. Conclusion

Accounting for varying target detectability can significantly improve tracking performance when these issues are present. The detectability can be estimated with a HMM based on the number of validated measurements, or the probability of the joint detectability and target existence may be jointly evaluated using the based on the likelihood ratio of a target vs. clutter. Simulations shows that both of these methods are able to maintain the track when the detectability is lowered, and terminates lost tracks significantly faster than a Markov chain 2-IPDA. Tests on real data shows that the joint estimation of target detectability and existence probabilities reduces the number of false tracks, at the cost of slightly higher track confirmation time.

Acknowledgment

This work was supported by the Research Council of Norway through project number 244116 and the Centres of Excellence funding scheme with project number 223254. Peter Willett was supported by AFOSR under contract FA9500-18-1-0463, and the professorship of Edmund Brekke has been funded by DNV GL. We would like to express great gratitude to Kongsberg Maritime and Maritime Robotics for providing the equipment and platforms used in the experiments.

References

[1] Y. Bar-Shalom, P. Willett, and X. Tian, *Tracking and Data Fusion: A Handbook of Algorithms*. YBS publishing Storrs, CT, USA, 2011.

[2] W. Blanding, P. Willett, Y. Bar-Shalom, and S. Coraluppi, "Multisensor Track Management for Targets with Fluctuating SNR," *IEEE Transactions on Aerospace and Electronic Systems*, vol. 45, no. 4, pp. 1275–1292, 2009.

[3] S. Colegrove and J. Ayliffe, "An Extension of Probabilistic Data Association to Include Track Initiation and Termination," in *Proc. of the 20th IREE International Convention*, 1985, pp. 853–856.

[4] B.-O. H. Eriksen, E. F. Wilthil, A. L. Flåten, E. Brekke, and M. Breivik, "Radar-based Maritime Collision Avoidance using Dynamic Window," in *Proc. of the IEEE Aerospace Conference*, March 2018.

[5] D. Kufoalor, E. F. Wilthil, I. Hagen, E. Brekke, and T. A. Johansen, "Autonomous COLREGs-Compliant Decision Making using Maritime Radar Tracking and Model Predictive Control," in *Proc. of the European Control Conference*, 2019.

[6] R. Mahler, *Advances in Statistical Multisource-Multitarget Information Fusion*. Artech House, 2014.

[7] R. Mahler, B.-T. Vo, and B.-N. Vo, "CPHD Filtering With Unknown Clutter Rate and Detection Profile," *IEEE Transactions on Signal Processing*, vol. 59, no. 8, pp. 3497–3513, 2011.

[8] D. Mušicki and R. Evans, "Joint Integrated Probabilistic Data Association: JIPDA," *IEEE transactions on Aerospace and Electronic Systems*, vol. 40, no. 3, pp. 1093–1099, 2004.

[9] D. Mušicki, R. Evans, and S. Stankovic, "Integrated Probabilistic Data Association," *IEEE Transactions on Automatic Control*, vol. 39, no. 6, pp. 1237–1241, Jun 1994.

[10] G. Papa, P. Braca, S. Horn, S. Marano, V. Matta, and P. Willett, "Multisensor Adaptive Bayesian Tracking Under Time-Varying Target Detection Probability," *IEEE Transactions on Aerospace and Electronic Systems*, vol. 52, no. 5, pp. 2193–2209, 2016.

[11] M. Schuster, M. Blaich, and J. Reuter, "Collision Avoidance for Vessels Using a Low-Cost Radar Sensor," in *Proc. of the 19th IFAC World Congress*, 2014, pp. 9673–9678.

[12] G. Soldi and P. Braca, "Online Estimation of Unknown Parameters in Multisensor-Multitarget Tracking: A Belief Propagation Approach," in *Proc. of the 21st International Conference on Information Fusion (FUSION)*, 2018.

[13] G. Van Keuk, "Sequential Track Extraction," *IEEE Transactions on Aerospace and Electronic Systems*, vol. 34, no. 4, pp. 1135–1148, 1998.

[14] J. L. Williams, "Marginal multi-Bernoulli Filters: RFS Derivation of MHT, JIPDA, and Association-Based MeMBer," *IEEE Transactions on Aerospace and Electronic Systems*, vol. 51, no. 3, pp. 1664–1687, 2015.

[15] E. F. Wilthil, E. Brekke, and O. B. Asplin, "Track Initiation for Maritime Radar Tracking with and without Prior Information," in *Proc. of the 21st International Conference on Information Fusion (FUSION)*, 2018.

[16] E. F. Wilthil, A. L. Flåten, and E. Brekke, "A Target Tracking System for ASV Collision Avoidance Based on the PDAF," in *Sensing and Control for Autonomous Vehicles: Applications to Land, Water and Air Vehicles*, T. I. Fossen, K. Y. Pettersen, and H. Nijmeijer, Eds. Springer International Publishing, 2017, pp. 269–288.